# Stress-induced microstructures and nanogaps embedded in plasmonic gratings

Sky Sun, Mido Kim, Juiena Hasan, and Sangho Bok\*\*

Abstract— Nanomaterials and nanostructures exhibit unique properties that are far different from bulk properties. Our group has utilized these unique properties to enhance signal performance in the detection of biomarkers for biosensing applications. Currently, we are developing metallic nanostructured sensor platforms to obtain ultrasensitive levels of detection. One useful property of metallic nanostructures, such as metallic nanogratings, is the ability to couple incident photons to a metallic/dielectric interface to form concentrated electromagnetic (EM) fields by surface plasmon resonance (SPR). When surrounding fluorescent dye molecules are exposed to these high intensity EM fields, the fluorescent emission intensity can be greatly enhanced to provide much better signal-to-noise ratios, reducing false positives, and improved detection limits, even down to single molecule detection.

Our group has been developing a modified microcontact printing process to inexpensively replicate the periodic structure of commercially available DVD discs and Blu-ray discs using polydimethylsiloxane (PDMS). The PDMS gratings are then coated with thin metals (e.g., gold films) to produce plasmonic gratings that can couple light at specific wavelengths and incidence angles, which appear as sharp dips in spectroscopic reflectivity measurements. In addition to the plasmonic gratings, we demonstrate a fabrication method to create additional structure and nanogaps in the plasmonic gratings. Controlled stress is applied to the plasmonic grating resulting in stress-induced structures in the plasmonic gratings. Different levels of stresses cause changes in physical properties of the structure including the sizes depths, and lengths of nanogaps. Nanogaps embedded in plasmonic gratings show much stronger SPR compared to plasmonic gratings without additional structure and nanogaps. Fabrication methods of creating the microstructure and nanogaps parallel to the gratings and perpendicular to the gratings are demonstrated as well as their characterization and properties.

# I. INTRODUCTION

The rising need for swift, affordable, and reliable diagnostic tools in personalized and point-of-care (POC) medicine provides opportunities for scientists to refine current technology platforms and create new techniques for detecting and quantifying clinically important biomarkers. Prompt diagnosis of infections and efficient disease control have always been crucial. Plasmonic-based biosensing offers a promising solution to the threat of diseases by enabling rapid disease monitoring. Recently, various plasmonic platforms have emerged, providing on-site strategies to supplement traditional diagnostic methods

Plasmonic biosensors are primarily categorized into two types: those utilizing thin metal-based films and those incorporating inorganic plasmon resonant nanostructures [3, 4]. One of the most widely recognized biosensors is surface plasmon resonance (SPR), which employs a metal-based film sensor, for analyzing biomolecular interactions [5]. These biosensors offer diverse sensing techniques, with some integrating both film-based and nanostructure platforms. Plasmon resonant nanostructures, whether used alone or in combination with film-based sensors, provide extensive sensing capabilities, making them indispensable tools in biosensing applications [6].

Metal nanostructures with nanogaps have been of special interest due to their ultra-strong electromagnetic fields and controllable optical properties, which can be useful for a variety of signal enhancements [7] such as spectroscopy, sensing, imaging, nonlinear optics, optical trapping, and metamaterials [8]. These applications benefit from the enhanced EM fields and directly transduce events of biomolecule-specific binding into electrical signals, such as changes in resistance, impedance, capacitance, dielectric properties, or field effect [7, 9]. The nanogap has been created in 1-D, 2-D, or 3-D structures to fulfill different requirements of applications [10]. The size of the nanogap fabrication is also controlled by the procedure method including mechanical break junctions, electron-beam lithography, electrochemical plating, electromigration, focused ion beam lithography, shadow mask evaporation, scanning probe and atomic force microscopy lithography, on-wire lithography, molecular rulers, etc. [11]. Here, we present an ongoing effort of fabricating controlled microstructure and nanogaps embedded gratings at low

such as polymerase chain reaction (PCR) and enzymelinked immunosorbent assays (ELISA) [1]. Disease detection can be achieved using a variety of plasmonic techniques, including propagating surface plasmon resonance (SPR), localized SPR (LSPR), surface-enhanced Raman scattering (SERS), surface-enhanced fluorescence (SEF), surface-enhanced infrared absorption spectroscopy, and plasmonic fluorescence sensors. The core components of a plasmonic sensor are the two types of surface plasmons (SPs): localized surface plasmons (LSPs) and propagating surface plasmon polaritons (SPPs) [2].

<sup>\*</sup>This material is based upon work supported by the National Science Foundation under Grant No. 2047894

<sup>\*\*</sup>S. Bok is with the Department of Electrical and Computer Engineering, University of Denver, Denver, CO 80208, USA (corresponding author, phone: 303-871-3752; email: sangho.bok@du.edu).

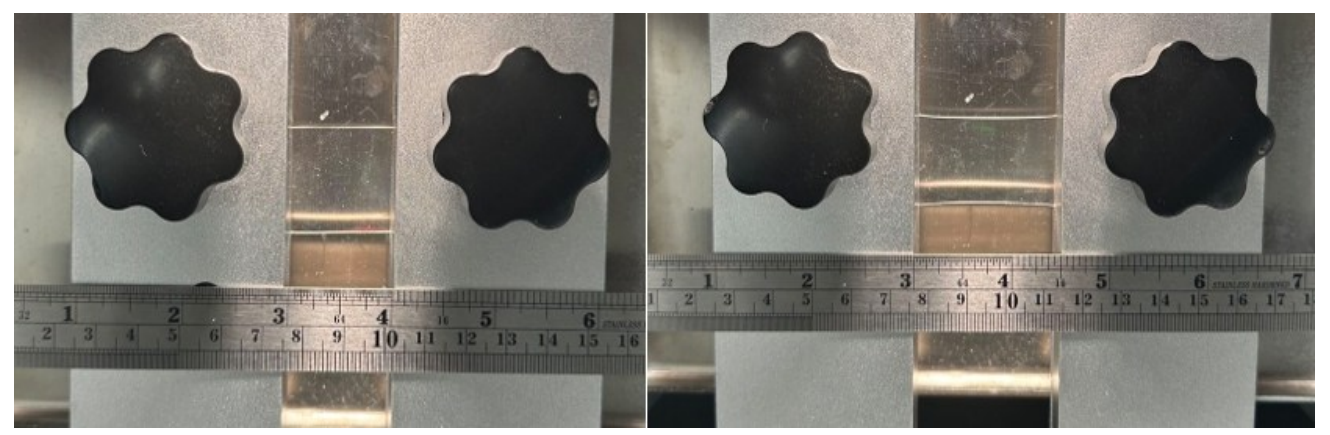


**Figure 1**. The experimental setup for the stress-induced PDMS gratings demonstrates the PDMS without stretching (left) and the 50% stretched PDMS (right).

## II. MATERIALS AND METHODS

# A. Sample preparation

## i. Fabrication of PDMS gratings

The PDMS gratings were fabricated by using a modified method from the previous studies [12, 13]. Briefly, the grating structure on DVD+R (Verbatim Americas LLC) was revealed by splitting the DVD disk in half by removing the side adhesion which was achieved by buffing the side with sandpapers followed by rinsing with DI water. The bottom half of disks with grating structures was rinsed with isopropanol (99% IPA, Lab Alley) for 2 minutes. The rinsing process with IPA was repeated until the solution was no longer blue. The metal films on the disk were removed by using 15% nitric acid for 15 min followed by rinsing with copious DI water. Once the metal films were removed, the disk were drying under flowing air. The cleaned disk was cast in 5: 1 base/cure agent of polydimethylsiloxane (PDMS) (Sylgard® 184 silicone, Dow Corning, Inc.) The disk coated in PDMS was placed at 24°C and 25% related humidity for 48 hours. The cured PDMS in the disk was cut into 1 X 1.5 inches for further processes.

#### ii. Stretching PDMS

Both ends of the longer edge for 0.25-inch were clamped on the workbench. The middle part was stretched till the length became 1.25 inches and 1.5 inches long (Fig 1). The structures were held for one hour and then released from the workbench. The PDMS was treated by oxygen plasma in a plasma system (PE 25-LF, Plasma Etch, Inc) for adhesion to a precleaned glass slide. The plasma treatment was performed for 90 seconds at 100 W with an oxygen flow rate of 10 cc/min [14].

## iii. Gold deposition

Gold (Au) films were deposited by using a sputtering system (ATC-2000 V, AJA International, Inc.). A 5 nm titanium (Ti) was deposited followed by Au deposition. A 100 nm gold layer was deposited using 100 W RF at a working pressure of 4 mTorr, ambient temperature (approximately 300 K). The deposition rates were 0.1 nm/s and 0.17 nm/s for Ti and Au, respectively.

## B. Characterization

The structures were examined under Scanning Electron Microscopy (SEM) by using ThermoScientific Volume Scope 2. The magnification and power were varied depending on the samples. The surface roughness was characterized by using an optical profilometer (Wyko Veeco NT 9109, Bruker). Root mean square (RMS) roughness was calculated at a 5x optical zoom with 2x digital zoom mode. Gwyddion (ver. 2.66) was used for the RMS surface roughness estimation.

### III. RESULT AND DISCUSSION

The structure of the Au coated PDMS gratings were characterized by using an SEM and an optical profilometer. The focus of the study was to examine the surface changes due to the stress caused by uniform stretch to the elastomer. The stretch was applied to the PDMS gratings in two different geometries. For the first PDMS grating set, the stretch was applied parallel to the gratings which created stress aligned with the grating lines (i.e., gratings with horizontal stress). For the second set, the stretch was applied perpendicular to the gratings, which created stress normal to the grating lines (i.e., gratings with vertical stress).

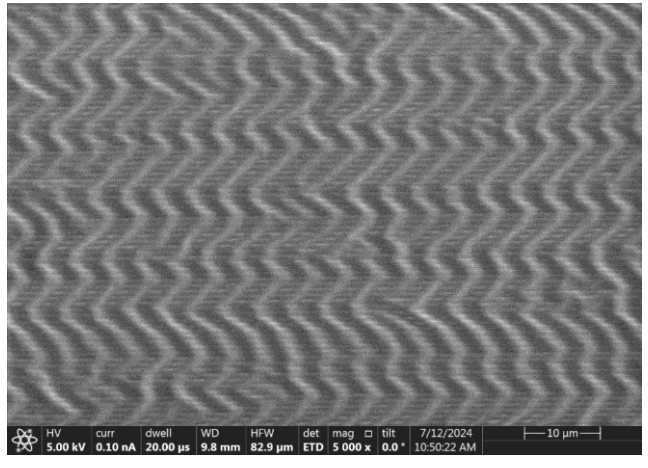


**Figure 2**. An SEM image for as-is gratings demonstrating the wavy microstructures (vertical lines) and gratings in the period of 740 nm (horizontal lines).

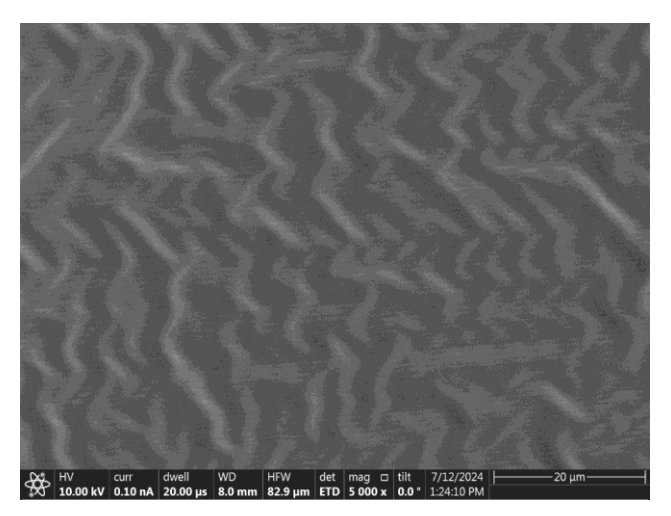


**Figure 3**. An SEM image for the gratings with horizontal stress demonstrating the disruption of the wavy microstructures.

For comparison, one set of gratings was prepared without any stretch (as-is gratings). The as-is gratings have shown the original grating lines in the period of 740 nm. Further, wavy periodic microstructures have been observed in the vertical direction to the gratings (Fig 2). After applying stress parallel to the gratings, the periodic microstructures were altered. In this case, the force was applied to the microstructures in 90°, disruptively (Fig 3), resulting in non-periodic microstructure embedded gratings. For the gratings with vertical stress, the microstructures looked undisrupted (Fig 4). However, this vertically applied force resulted in a smaller period for the microstructures and 10% reduction of the period was estimated.

The surface characteristics were further investigated by using the optical profilometer. The RMS surface roughness was  $178.7 \pm 4.8$  nm for the as-gratings. The RMS surface roughness was  $176.6 \pm 3.8$  nm and  $271.4 \pm 2.3$  nm for the gratings with vertical stress and the gratings with horizontal stress, respectively. The RMS surface roughness did not change significantly for the gratings with vertical stress while the surface roughness demonstrated a significant increase for the gratings with horizontal stress.

# IV. CONCLUSION

The analysis of SEM images and optical profilometer data reveals significant insights into the effects of stretching on PDMS gratings. The as-is gratings demonstrated periodic microstructures in addition to the gratings. The vertical stretching increased the density of the microstructures by 10 percent while the surface roughness did not increase. However, the horizontal stretching disrupted the microstructure resulting in the loss of periodicity while the surface roughness increased. The gratings structures transferred from the DVD+R served as a base structure. Previously, nanogaps have been created in similar gratings using stress [15]. Hence, nanogaps were expected to be created as this stretching process induced stress to the PDMS gratings. The SEM images did not show direct

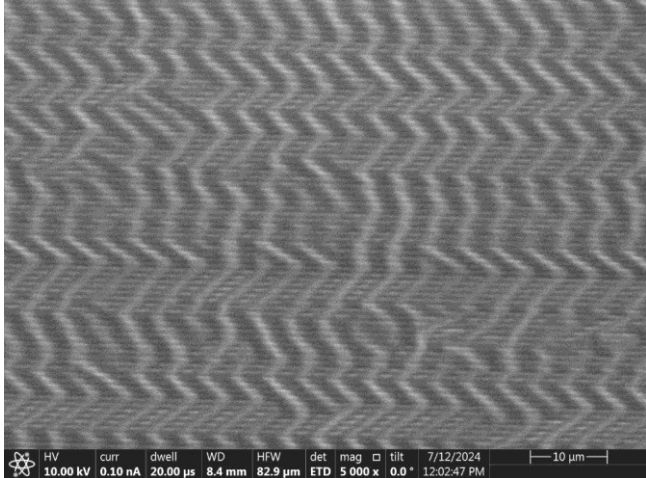


**Figure 4**. An SEM image for the gratings with vertical stress demonstrating the wavy microstructures (vertical lines) and gratings in the period of 740nm (horizontal lines).

evidence of the nanogaps, though. The current findings highlight the significant impact of stretching direction and magnitude on the surface morphology and roughness of PDMS gratings. The future work includes applications of the microstructure embedded gratings in biomedical sensors and investigation of nanogaps in higher resolution electron microscopy.

### REFERENCES

- Hasan, J., & Bok, S. (2024). Plasmonic Fluorescence Sensors in Diagnosis of Infectious Diseases. *Biosensors*, 14(3), 130. <a href="https://doi.org/10.3390/bios14030130">https://doi.org/10.3390/bios14030130</a>
- [2] Choi, I., & Choi, Y. (2011). Plasmonic nanosensors: review and prospect. IEEE Journal of Selected Topics in Quantum Electronics, 18(3), 1110-1121. DOI: <u>10.1109/JSTQE.2011.2163386</u>
- [3] Hamza, M. E., Othman, M. A., & Swillam, M. A. (2022).
   Plasmonic biosensors. Biology, 11(5), 621.
   <a href="https://doi.org/10.3390/biology11050621">https://doi.org/10.3390/biology11050621</a>
- [4] Mondal, B., & Zeng, S. (2021). Recent advances in Surface Plasmon Resonance for biosensing applications and future prospects. Nanophotonics in Biomedical Engineering, 21-48. <a href="https://doi.org/10.1007/978-981-15-6137-5">https://doi.org/10.1007/978-981-15-6137-5</a>
- [5] Miyazaki, C. M., Shimizu, F. M., & Ferreira, M. (2017). Surface plasmon resonance (SPR) for sensors and biosensors. In Nanocharacterization techniques (pp. 183-200). William Andrew Publishing. <a href="https://doi.org/10.1016/B978-0-323-49778-7.00006-0">https://doi.org/10.1016/B978-0-323-49778-7.00006-0</a>
- [6] Hill, R. T. (2015). Plasmonic biosensors. Wiley Interdisciplinary Reviews: Nanomedicine and Nanobiotechnology, 7(2), 152-168. https://doi.org/10.1002/wnan.1314
- [7] Nam, Jwa-Min, et al. "Plasmonic Nanogap-Enhanced Raman Scattering with Nanoparticles." Accounts of Chemical Research, vol. 49, no. 12, 2016, pp. 2746–55, <a href="https://doi.org/10.1021/acs.accounts.6b00409">https://doi.org/10.1021/acs.accounts.6b00409</a>.
- [8] Gu, Panpan, et al. "Plasmonic Nanogaps: From Fabrications to Optical Applications." Advanced Materials Interfaces, vol. 5, no. 19, 2018, https://doi.org/10.1002/admi.201800648.
- [9] Chen, Xing, et al. "Electrical Nanogap Devices for Biosensing." Materials Today (Kidlington, England), vol. 13, no. 11, 2010, pp. 28–41, https://doi.org/10.1016/S1369-7021(10)70201-7
- [10] Nevill, J. Tanner, and Daniele Malleo. "Nanogap Biosensors." Encyclopedia of Nanotechnology, Springer Netherlands, pp. 2384–93, <u>https://doi.org/10.1007/978-94-017-9780-1\_120</u>.

- [11] Li, Tao, et al. "Nanogap Electrodes." Advanced Materials (Weinheim), vol. 22, no. 2, 2010, pp. 286–300, <a href="https://doi.org/10.1002/adma.200900864">https://doi.org/10.1002/adma.200900864</a>.
- [12] Wood, A. J., et al. "Influence of Silver Grain Size, Roughness, and Profile on the Extraordinary Fluorescence Enhancement Capabilities of Grating Coupled Surface Plasmon Resonance." RSC Advances, vol. 5, no. 96, 2015, pp. 78534–44, https://doi.org/10.1039/C5RA17228D.
- [13] Chen, B., et al. "Plasmonic Gratings with Nano-Protrusions Made by Glancing Angle Deposition for Single-Molecule Super-Resolution Imaging." Nanoscale, vol. 8, no. 24, 2016, pp. 12189–201, <a href="https://doi.org/10.1039/c5nr09165a">https://doi.org/10.1039/c5nr09165a</a>.
  [14] Hill, S., Qian, W., Chen, W., & Fu, J. (2016). Surface
- [14] Hill, S., Qian, W., Chen, W., & Fu, J. (2016). Surface micromachining of polydimethylsiloxane for microfluidics applications. Biomicrofluidics, 10(5). https://doi.org/10.1063/1.4964717
- [15] Wood, A. J., et al. "Enhanced DNA Detection Through the Incorporation of Nanocones and Cavities into a Plasmonic Grating Sensor Platform", IEEE Sensors Journal, vol. 16, no. 10, pp. 3403-3408, 2016, https://doi.org/10.1109/JSEN.2015.2479473